Acoustic microscopy

Electroacoustical transducers and acoustic lenses work at megahertz frequencies as "miniature sonar systems," forming high-resolution images that show properties not seen in optical micrographs.

Calvin F. Quate

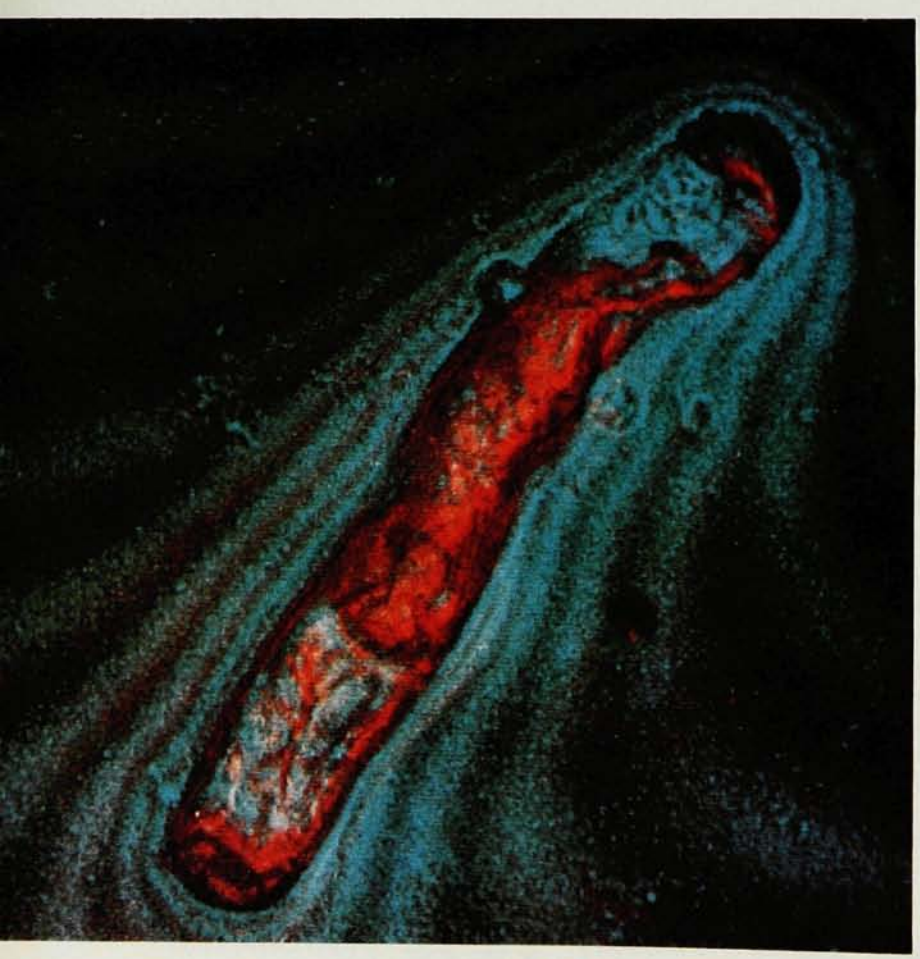

The acoustic microscope is a new entry in the field of microscopic imaging. It comes after a delay of many years, but now appears to be well established. At last year's conference of the Royal Microscopical Society in London, for example, the booth traditionally reserved for new instruments was used to introduce commercial versions of acoustic instruments.[1] Visitors to the exhibit learned that one can focus acoustic waves in water to a diffraction-limited waist and use them as a probe for microscopic examination. They found in examining their own samples that they could observe new detail with a resolution comparable to that achieved by optical microscopes. (See figures 1 and 2.)

It is not easy to explain the delay in the introduction of acoustics into microscopy. Much of the technology has been around for some time. The idea surfaced in the Soviet Union as early as 1949, when Sergei Y. Sokolov pointed out[2] that the wavelength of 3-GHz sound in water is equal to the wavelength of green light. He suggested that an imaging system at that frequency might compete with optical instruments. There were some attempts[3] in this direction in 1960, but the serious work on acoustic microscopy did not start until the late 1960s. At the Zenith Laboratory in Chicago,

0031-9228 / 85 /

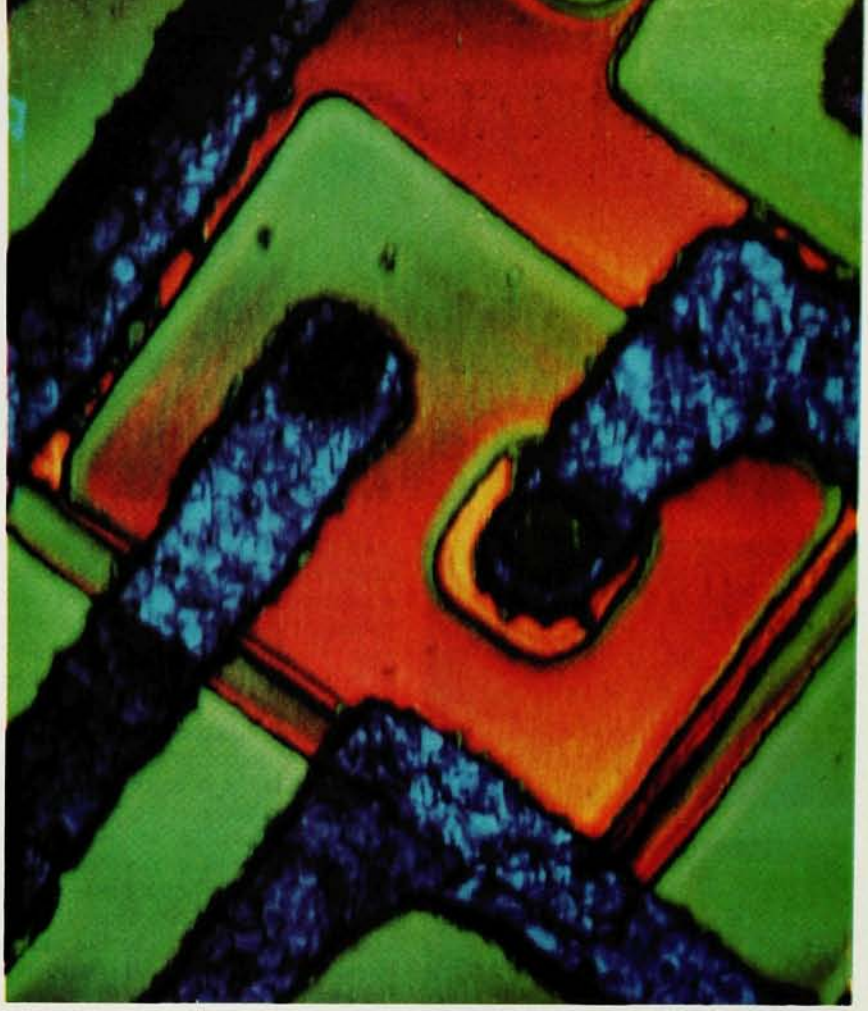

Acoustic micrographs. Right: Image of a bipolar transistor. The connecting lines are made of aluminum and are 2 microns wide. Opposite page: Acoustic image of a myxobacterium, which is a member of a social spore-forming class of bacteria. The diameter of the bacterium is 0.5 microns. (Bipolar transistor courtesy of TRW Inc.) Figure 1

Larry Kessler and Adrian Korpel developed an acoustic system in which a scanned laser beam reads the image from a plastic membrane deformed by the acoustic signal. At Stanford, Bertram Auld and his students demonstrated and analyzed several systems of microscopic acoustic imaging. These workers and others in that early period established many of the basic principles of acoustic microscopy, and their work influenced all that followed.

In this article I discuss the physics of acoustic microscopy and consider the technique's applications and potential for further development. While I draw many of my examples from our research program at Stanford, excellent work on acoustic microscopy is under way all over the world. At Tokohu University in Sendai, Japan, a group under the leadership of Noriyoshi Chubachi has shown how to get quantitative information from the character of acoustic pulses reflected from samples. At the Université des Sciences et Techniques du Languedoc, in Montpellier, France, Jacques Attal has demonstrated how one can get information from the interiors of solids. At University College London, Eric Ash's acoustic imaging group has made effective use of the phase information in acoustic reflections to obtain contrast and to do internal imaging. And at the General Electric Company in Schenectady, New York, Robert Gilmore has pioneered the use of low frequencies for scanning in depth over large surfaces. Scientists elsewhere have built instruments to demonstrate other characteristics of acoustic imaging; a special issue[4] of the *IEEE Transactions on Sonics and Ultrasonics* gives a more complete description of their work.

The advent of acoustic microscopy is only part of the renaissance that is taking place in the field of imaging. Other new instruments are using ion beams,[5] tunneling electrons[6] and x rays to study the microscopic world (see the article in this issue on x-ray microscopy, page 22, and the article on x-ray optics, April 1984, page 44). The table on page 36 compares the resolving powers of the various instruments. The new probes challenge the dominant position of optical waves and electron beams, but it is unlikely that the conventional methods will be displaced, as each viewing instrument extracts different information from the specimen. The ion microscope is powerful because it can analyze the masses of atomic species that come from the specimen during sputtering. The tunneling microscope allows us to study surfaces on an atomic scale, and is bound to have a large impact in surface science. The scanning x-ray microscope has the potential for far greater resolution, and this will be realized as aberrations in x-ray lenses are corrected.

The acoustic system

The acoustic microscope differs from optical instruments in several significant ways. The change from optical to acoustic energy allows us to use frequencies in the microwave region. We must use a different kind of lens for focusing. We can not use photographic film, but must rely on piezoelectric transducers and electronic detectors. In combination these differences give us a new instrument, an instrument that extends our capability for observation beyond the limit set by optical systems.

We can operate the acoustic instrument at 3 MHz in water, where the wavelength is 500 microns, and at 8 GHz in helium, where the wavelength is 300 Å. This wavelength range, exceeding four orders of magnitude, is equivalent to operating an optical system from the microwave region, through the infrared, through the visible and beyond the vacuum ultraviolet.

Calvin Quate is professor in the departments of applied physics and electrical engineering at Stanford University. He is a senior research fellow at the Xerox Palo Alto Research Center.

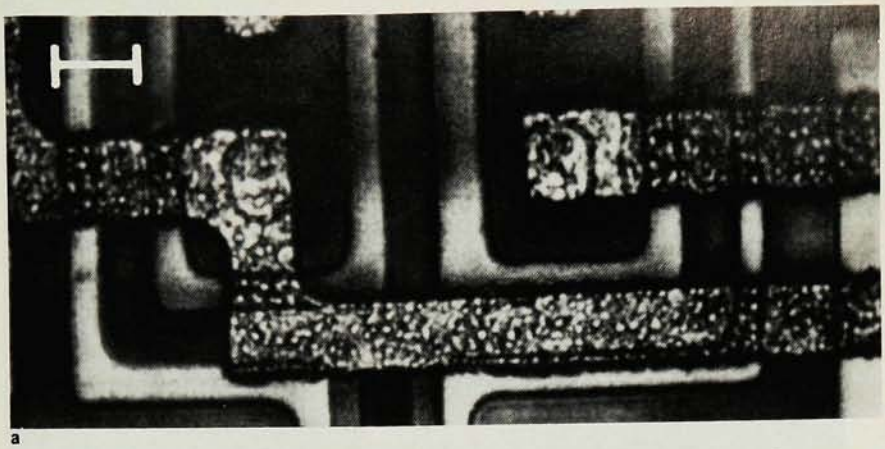

a

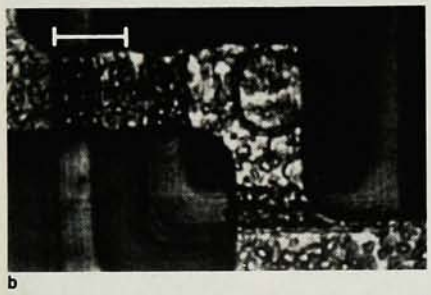

b

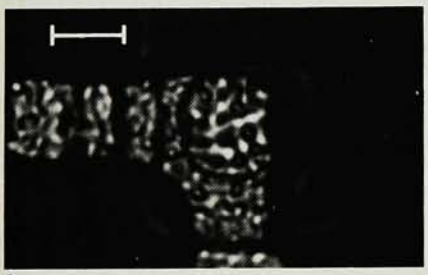

c

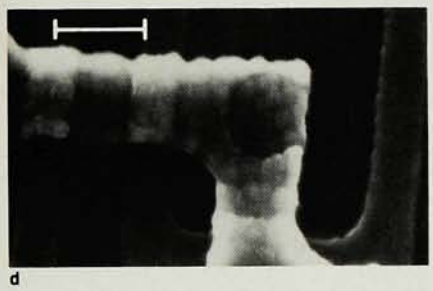

d

Comparison of micrographs. **a:** Acoustic image of bipolar transistors on a silicon integrated circuit. **b:** High-magnification acoustic image of the base contact of a transistor. **c:** Optical micrograph of the same area as in **b**. **d:** Scanning electron micrograph of the same area. Scale bars represent a distance of 3 microns. (Images by Babur Hadimioglu, ref. 12.) Figure 2

Furthermore, the piezoelectric detectors permit us to exploit coherent radiation, where information is available from both the amplitude and phase of the reflected signals. The piezoelectric films, typically made from zinc oxide, are efficient. As generators these films can convert 50% of the electromagnetic energy into sound. As detectors they can convert 50% of the sound into electromagnetic energy.

The lens is the heart of the acoustic microscope. It is deceptively simple, but it makes all the difference in the imaging work. The lens can have various forms, such as the one shown in figure 3a, which is a sketch of a lens that we have used at high frequencies at Stanford. The lens is a sapphire crystal with a spherical cavity; it is immersed in a fluid that makes contact with the specimen. When a plane wave of sound is launched into this crystal by a piezoelectric film, it is converted to a spherical wave at the solid–liquid interface. Focusing, limited only by diffraction, is easily obtained with this single-surface lens.

There are no aberrations because the velocity of sound in the fiuid is small compared to the velocity of sound in the solid, and therefore there is a large angle of refraction at the interface. The direction of a ray crossing the interface into the liquid lies close to the normal. In this situation the focal length is nearly equal to the radius of curvature of the surface and the spherical aberrations are reduced to negligible values. There is, of course, a penalty. The change in velocity is accompanied by a strong discontinuity in the acoustic impedance, a problem that must be overcome to transfer energy efficiently into the liquid. We have found that a layer of carbon makes an excellent antireflection coating.

An acoustic-microscope system resembles a miniature radar or sonar system. The acoustic beam, after reflection from the sample, passes back through the lens and into the piezoelectric transducer that generated it. The transducer, now working as a receiver, detects the signal, whose amplitude and phase carry information about the sample. The acoustic lens moves in a raster pattern over the specimen, examining each point sequentially. The system requires several seconds to cover a single frame containing 512×512 pixels, each of which is typically 0.5 microns in size. The returning pulses modulate the intensity of the beam in a cathode-ray-tube monitor. The display system is similar to that in a scanning electron microscope.

The interface wave

What is it that we "see" in acoustic images that we do not "see" in optical images? Here are a few representative examples: We can see fibers inside various composite materials; we can see features of biological cells that are difficult to image in the optical microscope; and we can see contrast that tells us about the structure and the adhesive properties of metal films and other coatings. Abrupt changes in elastic properties show up in acoustic micrographs where there are no corresponding changes in the optical index of refraction. For example, with polycrystalline samples of anisotropic metals, the optical image of a polished surface is smooth and featureless. In the acoustic images, individual grains stand out, showing their random orientations.

There is contrast between individual grains and their neighbors because there is a wave that travels along the interface between the sample and the overlying liquid, and this "interface wave" is sensitive to small variations in the elasticity of the exposed surface. The interface wave is responsible for highlighting the elastic properties, or rather the changes in these properties, in acoustic images. Surface waves of this type, common in acoustic systems, have no counterpart in electromagnetic systems. When we first encountered them in our work we were unprepared for the remarkable changes that they produce in images when the sample is moved away from the focal plane, toward the lens.

The effect of this defocusing is most easily demonstrated by measuring the output voltage V from the transducers while varying the lens-to-sample spacing z. In this measurement, one suppresses the lateral translation of the sample so that the output is a single curve of voltage versus spacing. For a classical focusing system with coherent

Scanning instruments

Technique	Resolution
Optical microscopy	2000 Å
X-ray microscopy	500–700 Å
Ion microscopy	400 Å
Acoustic microscopy	200 Å
Tunneling microscopy	2 Å

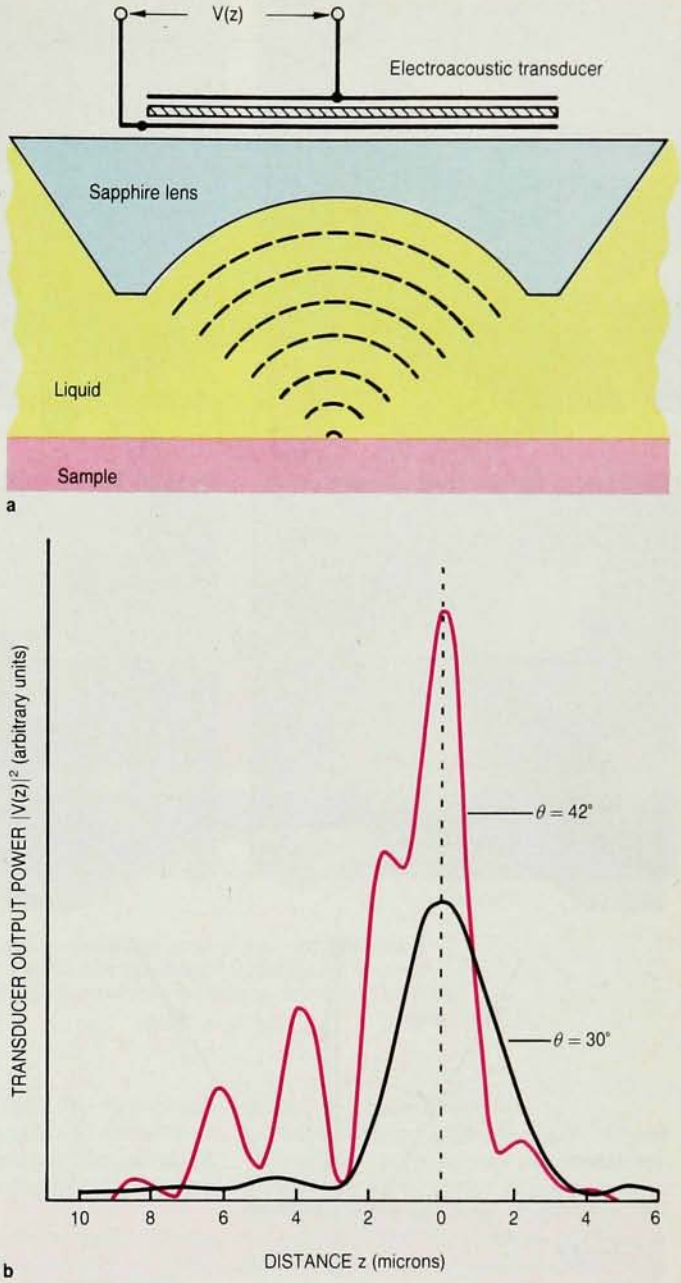

Lens configuration (**a**) and transducer output (**b**). The lens is a spherical cavity in sapphire. The plots show the measured transducer output power as a function of the distance between the lens and an aluminum specimen in water at about 40° C. The acoustic frequency is 1.8 GHz. The angle θ is the opening angle of the acoustic lens used to collect the data. Figure 3

radiation and a phase-sensitive detector, the voltage curve has the form $\sin z/z$. In an acoustic system with a small-aperture lens, these surface waves are not excited and we do indeed measure such a curve. The experimental curves in figure 3b, recorded at Stanford by Larry Lam, demonstrate this point. The sample was aluminum with a polished surface, and the working fluid was water. For these materials, the critical angle for coupling to the interface wave is 33°. The opening angle for the lens used to collect the data represented by one of the curves is 30°, which is less than the critical angle. The interface wave is not excited and the classical $\sin z/z$ curve is the result. The other curve shows the response for a lens with an opening angle of 42°, which is large enough to encompass the critical angle. The form of this response curve is fundamentally different because the surface wave is now generated. The deep minima come from the interference between the ray at normal incidence and the ray at the critical angle.

We can clarify this interference still further by reference to figure 4. The transducer depicted at the top of the figure is a piezoelectric film that generates short pulses of acoustic energy. Each pulse is a plane wave of sound that propagates downward through the crystal into the liquid. As the wave passes through the surface of the lens, it is transformed into a spherical wave that converges toward a focal point. After reflecting from the sample, the acoustic pulse returns through the lens to the transducer, which converts it back to an electrical pulse that is the output signal.

This system has a very small field of view. This means that the transducer responds only to those rays that appear to be reflected from a small region very near the focal point of the lens. When the surface of the reflecting sample is placed near the focal plane, the entire beam is reflected and the transducer output is maximized. When the surface of the reflecting sample is displaced from the focal plane, it still reflects much of the beam, but in such a way that it appears to come from a region far from the focal point. The transducer does not respond to those rays because they do not meet it at normal incidence. The transducer can only respond to a narrow central cone, because that cone always meets it at normal incidence. That cone, marked A in figure 4a, appears to originate in the focal plane regardless of the position of the reflecting sample. There is, however, a second mechanism by which reflected rays can appear to come from the focal plane. This involves the surface wave produced by the incoming radiation that meets the interface at the critical angle. The surface wave travels along the interface and continually reradiates energy back into the liquid at the same critical angle. The ray marked B in figure 4a illustrates this. The direction of this ray makes it indistinguishable from a ray reflected from the focal plane.

The two components represented by the ray paths marked A and B in figure 4b contribute to the transducer output with an amplitude that is nearly independent of the position of the reflecting sample. There is a phase shift between the two components, and this sets up an interference pattern that changes when the lens-to-sample spacing is varied. The distance between minima in this interference pattern measures the velocity of the interface wave along the surface of the sample. This, in turn, tells us something about the elastic properties of the sample. The pattern of interference illustrates the variation in elastic constants over the

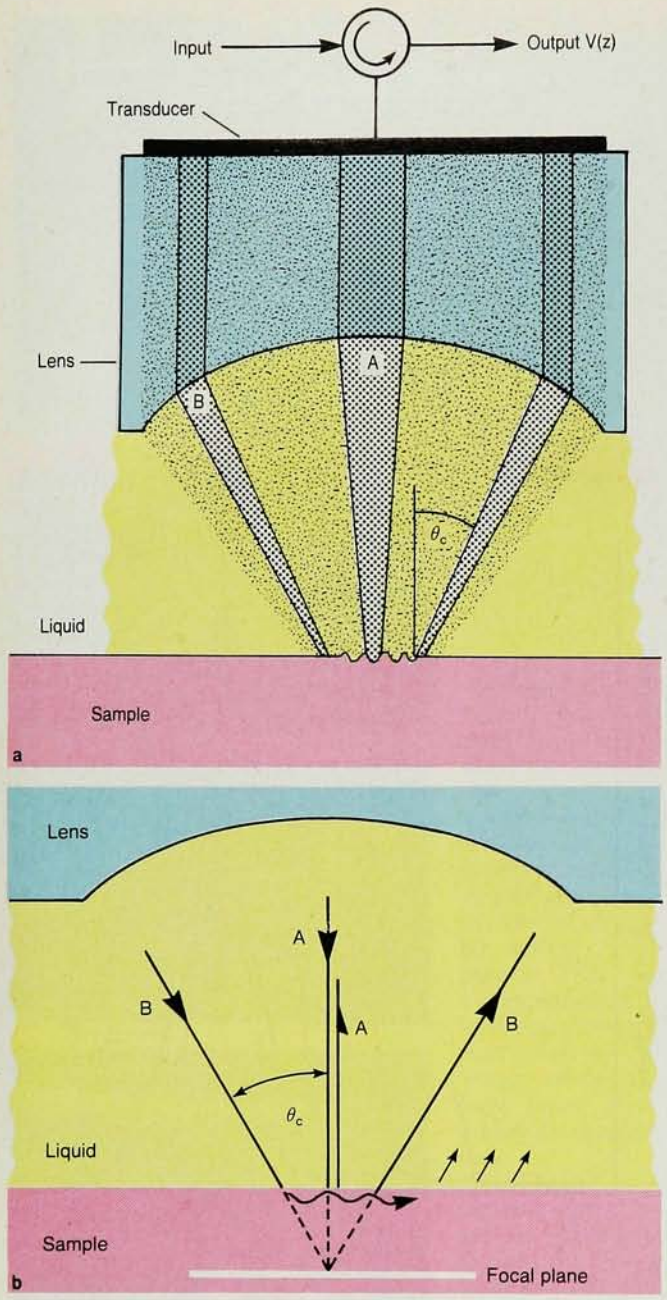

Ray paths and interference scheme. a: Sketch of the transducer–lens system emphasizing the central cone and the critical-angle cone. **b:** Ray diagram showing the paths of the two acoustic signals that interfere at the transducer and generate the $V(z)$ curve. Figure 4

surface of the sample and provides the contrast that we record in the display.

History of the $V(z)$ effect

The interference between the central cone and the surface wave produces remarkable images. Robert Wilson at Hughes Research Laboratories, working with Rolf Weglein, once sat on a high stool for hour upon hour and recorded acoustic images as he moved the sample toward the lens in discrete intervals.[7] That series was pivotal; the striking regularities were difficult to explain with any model that anyone was using. In our own lab, Abdullah Atalar, who first introduced the reflection instrument while he was a graduate student, tried in vain to tell us that there might be new information in his out-of-focus images.[8] We were inclined to attribute the changes to aberrations in the lens. It was only after he recorded images of the grains in an alloy of nickel that we were convinced.

At that point we knew that the changes in contrast depend on the nature of the sample. We realized for the first time that we might use the $V(z)$ effect to image the elastic properties of materials, and we began work in earnest. We found that one can clearly delineate the grain structure of metals and ceramics, and that one can study subsurface structures if they are within reach of the interface wave, which extends about one wavelength into the solid. This distance is 8 microns in silicon at 1 GHz, and 2 microns at 4 GHz.

We set about the task of correcting our model. In the process, we uncovered the work[9] of Mack Breazeale at the University of Tennessee, who had characterized steel samples by exploiting the fact that acoustic waves reflected from a liquid–solid interface are displaced laterally, an effect known as the Schoch displacement. Kumar Wickramasinghe, now at IBM, calculated[10] the transducer output voltage V as a function of the lens-to-sample spacing z—the $V(z)$ curve—in a concise manner, providing additional insight into this important and distinctive source of contrast. Henry Bertoni of the Polytechnic Institute of New York published[11] a ray theory that also increases our understanding of the interactions that take place in the out-of-focus geometry.

The recorded images, which I will now consider, illustrate what can now be done with acoustic microscopy.

The images

The texture, or grain structure, of polycrystalline materials is the first and most dramatic difference that shows up in comparisons of acoustical and optical images. Inconel and titanium samples illustrate these differences. We see in figures 5a and 5b contrast changes from grain to grain. We don't yet fully understand the source of the contrast that highlights the boundaries. That remains as a problem for the commercial instruments to unravel. Figure 6 shows state-of-the-art images from commercial instruments. The detail and contrast in these images, of aluminum lines on silicon and of glass fibers embedded in epoxy, demonstrate the power of electronics in presenting images.

Integrated circuits, with their dominant role in today's technology, require better and better performance from imaging instruments. Acoustic imaging should play a role in selected areas such as the problem of achieving adhesion in the deposition of thin films. Photomasks for the fabrication of integrated circuits are commonly made of

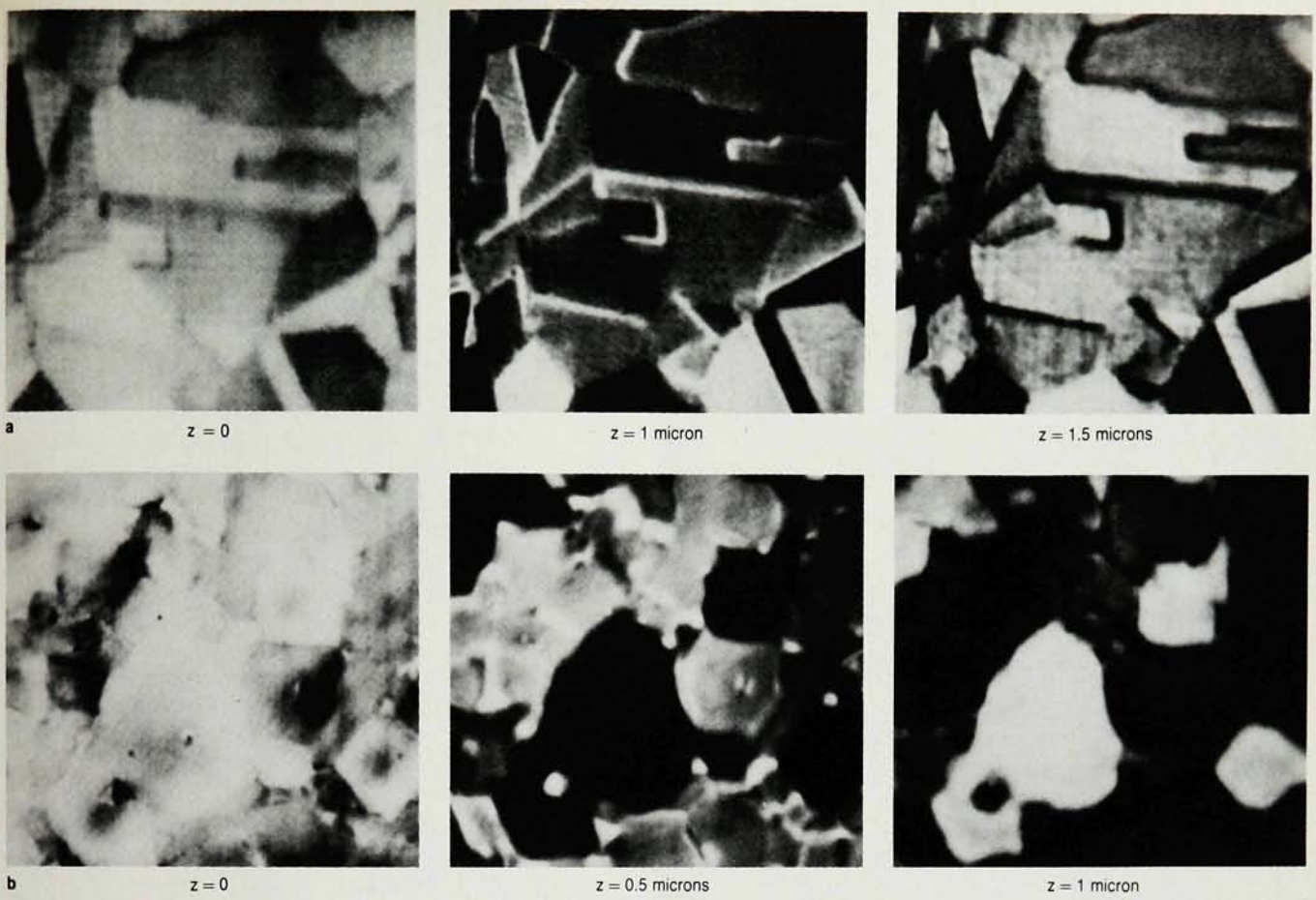

Contrast enhancement. a: Three images of a polished inconel surface, showing the grain structure with increasing contrast as the sample is moved from the focal plane ($z = 0$) toward the lens. The operating frequency is 1.8 GHz. The rectangular area imaged is about 80 microns wide. **b:** Acoustic images of a polished surface of titanium. The area imaged is about 70 microns wide. Figure 5

chrome on glass. The lack of adhesion of the chrome films is a serious defect that is difficult to identify with optical methods.

Heat dissipation in integrated-circuit chips is another area where acoustics will be important. Chips must be securely bonded to their heat sinks, and manufacturers require some method for monitoring this bond. The solder used for bonding often contains voids and fissures that reduce the heat conductivity to unacceptable levels. Acoustic instruments that operate at moderate frequencies with reduced resolution can now monitor problems of this kind.

The remarkable penetrating power of acoustic radiation is demonstrated in the work of Butrus Khuri-Yakub at Stanford. In one experiment, he used a lens in the form of a spherical shell in an instrument operating at a frequency of 3 MHz—a wavelength of 500 microns—to image a honeycomb structure used as the skin of aircraft. The structure consists of two sheets of aluminum held apart by a honeycomb grid. He can either focus on the surface, which gives a bland, uninteresting image, or on the internal structure. The internal image with the hexagonal grid illustrates the unique feature of acoustic imaging because the inside of the sample is inaccessible to optical radiation.

Polymers such as those used to make photoresist patterns represent another area of opportunity for acoustic imaging. Photoresist material can be troublesome if for some reason it contains defects such as bubbles. Lack of contrast in optical images hides these defects, but in acoustic images they appear as points of strong reflection.

In polymer materials, both the velocity of sound and the acoustic impedance have values quite close to those of water, which is the working fluid between the lens and the sample. We do not observe the $V(z)$ effect in these materials because the critical angle is too large. However, the reflection at the interface is small, and this allows the acoustic beam to propagate into the interior. Inclusions and other defects are prominent features in the images. The inclusions that appear deep inside the film have impedances that are much less than that of the surrounding polymer. It is easy to identify small pockets of gel, which are a common defect in these films.

Distributing high-strength fibers throughout polymers or other materials strengthens those materials and modifies some of their other physical properties. The distribution of fibers is difficult to monitor with optical radiation because the host material is often opaque. In an acoustic field, the fibers produce strong reflections because their acoustic impedance is higher than that of the host material. Figure 7 shows an example of an image in which glass fibers are the only apparent feature. It is in some sense a "binary" image, with two values, black and white.

Finally, we return to the high-magnification acoustic image shown in figure 2. This image, taken with an acoustic microscope operating at 4.5 GHz, rivals optical images in quality and resolution. It represents the high point for acoustic imaging in water.

Biology. Biological cells represent a class of objects that are entirely different from the solid objects discussed above. Optical absorption is not large in these cells, so optical imaging requires special techniques such as differential interference contrast. Acoustic

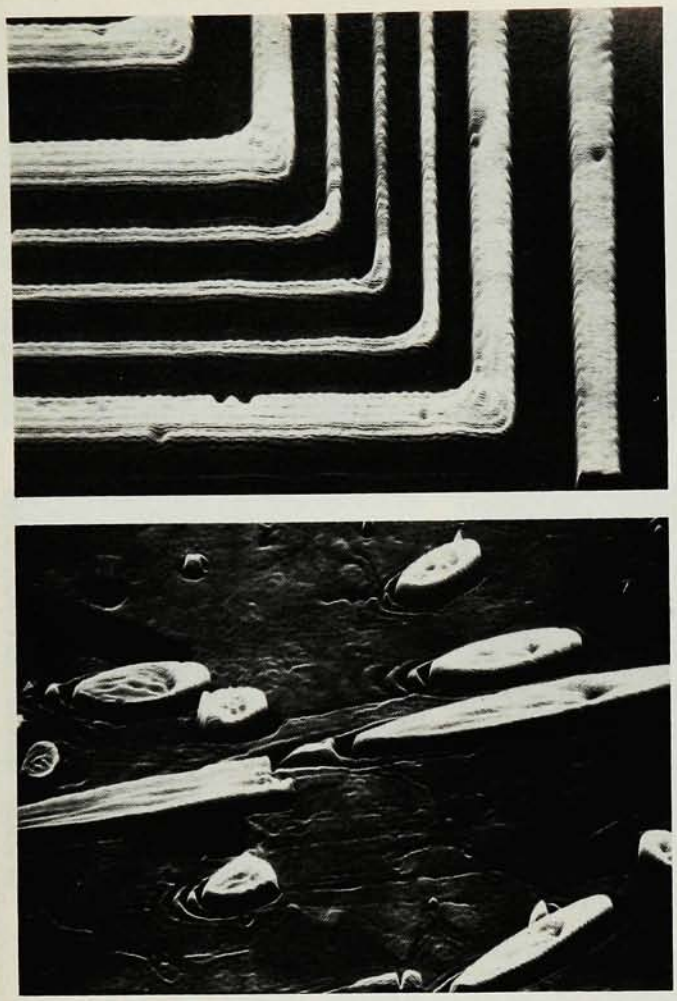

Highlighting in images produced by a commercial acoustic microscope. Top: Aluminum lines on silicon. The aluminum line at the right is about 6 microns wide. Bottom: Glass fibers embedded in epoxy. (Courtesy of E. Leitz Inc.) Figure 6

micrographs serve to increase the contrast in biological samples and to bring out new details. Sound waves travel through the entire cell with ease because cellular material is largely water. Nevertheless, there are differences in the acoustic properties of the cellular material, and these represent sources of contrast in the images.

With cells grown on glass substrates, we encounter two reflections, one at the liquid–cell interface at the top of the cell, and the other at the cell–substrate interface beneath the cell. These reflections interfere constructively or destructively as the cell thickness varies. Contours of constant cell thickness appear as dark rings. Changes in the ring structure allow us to study the dynamic properties of the cell. Such features as adhesion to the substrate, movement of particles, and construction and deconstruction of filaments through polymerization and depolymerization are easily observed.[13] New information on cellular movement should be forthcoming from acoustic microscopy.

The changes in elastic properties that take place in cells and tissues should also show up in acoustic micrographs, although the evidence to support this hunch is not yet available.[14] Imaging such changes would be useful for studying pathological specimens.

Resolving power

Each instrument used for microscopic imaging has features that make it unique and interesting. However, it is an instrument's resolving power, as listed in the table on page 36, that determines where it will be used. The useful operating range for optics is limited by the large absorption in the ultraviolet region. As a rule of thumb, the resolution of the conventional optical microscope is 0.4 microns in air, 0.3 microns in water and 0.2 microns in oil. These numbers set the goals for competing instruments.

In a similar way, it is acoustic absorption in liquids that limits the upper operating frequencies of the acoustic microscope. Sound absorption per unit distance increases as the square of the frequency. If we use wavelengths shorter than those of microwave frequencies, we encounter severe restraints. The electronics dictate that to preserve an acceptable signal-to-noise ratio we must maintain the total attenuation along the signal path at a constant level. If we double the frequency, for example, we must reduce the signal path to one-quarter its previous length. The lenses must be fabricated with smaller and smaller radii.

We have been able to achieve a signal-to-noise ratio of 30 dB at 4.5 GHz with a lens 16 microns in radius. This gives a resolution near 0.2 microns (see figure 2), the limit of the optical microscope.

If we seek to improve the resolution to observe objects below that size, we must use a liquid with an acoustic velocity less than that of water. There are such liquids at room temperature, but they are not useful because their attenuation is too large. Cryoliquids emerge as the most attractive candidates.

Liquid nitrogen is a convenient and readily available cryofluid. The absorption of sound in this liquid is similar to that in water, while the velocity of sound is one-half that in water. At a given frequency, we can improve the resolution by a factor of two by transferring the instrument from water to liquid nitrogen.

While working with liquid nitrogen, Daniel Rugar, now at IBM San Jose, discovered[15] a new phenomenon that is important for imaging. He found that one can improve the resolution by moving to the nonlinear regime, where the amplitude of the sound wave is high enough to generate harmonics. While the evidence is clear—images with improved resolution—the theoretical explanation is less clear. The improvement may come from second harmonics, because those components produce a sharper image than the fundamental frequency. However, there seems to be a dilemma. How can one observe the second harmonic content by monitoring the output with a detector that operates at the fundamental frequency? The theory that has been published shows that this is indeed reasonable and that the behavior of nonlinear waves in spherically focused beams is quite different from what we expected, but we don't yet have a simple description that I can present here.

Liquid helium. The ultimate resolution with acoustics will come from an instrument immersed in liquid helium. In this liquid the sound velocity is one-sixth of that in water and the absorption of sound decreases with the fourth power of the temperature when the

Torr Master® Cryopumps...
Designed for performance, reliability, and field service

What everyone wants from their ultra-high vacuum source is faster pumpdown time and a longer time between regenerations. Here's how Torr Master® superior design can help you achieve these goals.

Performance. For example, compare the performance of our TM150 8-inch cryopump with those of other manufacturers.

- Pumping speeds improved 9%
- Pumping capacity improved 8%
- Refrigeration capacity improved 20%
- Argon throughput capacity improved 8%
- Hydrogen capacity improved 60%

Reliability. Key to the dependability of our cryopumps is design simplicity—fewer moving parts in compressor and cold head, no O-ring seals on any moving components, and no moving parts or working fluids exposed to vacuum. We use the finest materials, such as filled polymer bearing surfaces to reduce wear. And, we back every cryopump we sell with an 18-month limited warranty.

Field Service. When maintenance is necessary, the work can usually be done in your plant. No special tools are required for assembly or disassembly and no alignments or adjustments of components are necessary. When other cryopumps fail, they may require special tools or skills or have to be sent back to the manufacturer. Our field serviceability can save you hours of production time.

Call or write for our full-line Torr Master® brochure describing each cryopump model (8″ to 20″), compressors, and accessories. Before you buy, compare Torr Master® performance and reliability.

CVI Incorporated

P.O. Box 2138
Columbus, Ohio 43216
614/876-7381

2975 Airway
Costa Mesa, California 92626
714/966-0731

Circle number 20 on Reader Service Card

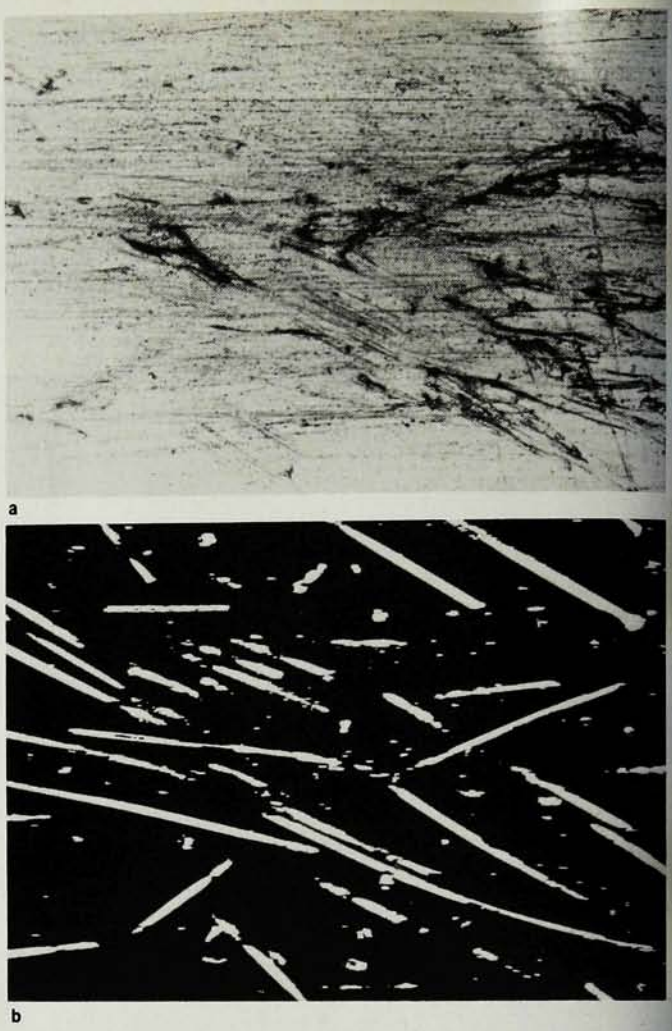

Glass-reinforced polymer. a: Optical-microscope image. **b:** Acoustic-microscope image produced with 0.9-GHz acoustic radiation. The width of the area imaged is 400 microns. (Courtesy of Mark Hoppe, E. Leitz Inc.) Figure 7

liquid is cooled well below the lambda point. When we operate at 100 mK, for example, the absorption is reduced to the point where it is no longer a limitation on the operating frequency.[16]

The behavior of this liquid baffled us for a time because we could not find the signal reflected from the object. At first we thought it was either a problem of misalignment or a lack of input signal strength. Hence, that is what we worked on—new methods of alignment, efficient transducers, antireflection coatings. We injected higher and higher levels of sound power into the liquid helium in an effort to increase the strength of the reflected signal, but our efforts were in vain, for they never produced a signal.

It took us a very long time to get all of this straight. We now know that the culprit is the nonlinear behavior of the medium. This behavior is emphasized when the intensity is increased by focusing the beam, but it is worse than that. We have learned that increasing the input level of a focused beam above a certain intensity can actually reduce the energy at the fundamental frequency. The energy is effectively lost when it is transferred to the higher harmonic frequency because the piezoelectric detector is unable to respond to the shifted frequencies.

The levels that we commonly use in present-day instruments are 30 dB below the levels that we used in the dark days when there were no signals. We have been forced to use every known strategy to capture and manipulate the weak signals. We have learned from the radioastronomers how to build GaAs FET amplifiers cooled to 4 K to achieve low effective noise temperatures. We have learned from the radar community how to employ chirped signals to lower the peak power levels of input without sacrificing the total energy.

With all of these improvements, our system appears to be working rather well.[17] We produce images at two frequencies—4.2 GHz and 8.0 GHz. At 4.2 GHz the wavelength is 570 Å and the resolution is near 400 Å. The image of the integrated circuit in figure 1 is a typical example. The sample is a bipolar transistor with a line width of 2 microns. The depth of focus for the acoustic beam is approximately 1500 Å, less than the height of the aluminum lines. We are able to record several images—each focused on a different level. We then assign each image a different color and assemble them into a composite with a computer. Thus color in the figure represents height in the object.

When we operate at 8 GHz, where the wavelength is 310 Å, the resolution appears to be better than 200 Å. The most interesting result is the image of a specimen of myxobacteria furnished to us by Stanford biochemist Dale Kaiser. The contrast in the composite image, shown in figure 1, is much greater than that found in a transmission-electron-microscope image.

This result suggests that the helium acoustic microscope, with its narrow depth of focus that makes the surface topology show up with high contrast, will one day play a role in the study of microscopic objects.

* * *

My work on acoustic microscopy is supported in part by the National Science Foundation and the Air Force Office of Scientific Research, and, in the past, by the Office of Naval Research.

References

1. Proc. Roy. Microscopical Soc. **19**, Part 4, MICRO 84 Supplement (July 1984).
2. S. Y. Sokolov, Dokl. Akad. Nauk. SSSR **64**, 333 (1949).
3. G. L. Clark, ed., *The Encyclopedia of Microscopy*, Reinhold, New York (1962), p. 544.
4. IEEE Trans. Sonics Ultrason. **SU-32**, No. 2 (1985).
5. A. L. Robinson, Science **225**, 1137 (1984).
6. G. Binnig, H. Rohrer, Ch. Gerber, E. Weibel, Phys. Rev. Lett. **50**, 120 (1983).
7. R. G. Wilson, R. D. Weglein, J. Appl. Phys. **55**, 3261 (1984).
8. A. Atalar, J. Appl. Phys. **50**, 8237 (1979).
9. M. A. Breazeale, L. Adler, G. W. Scott, J. Appl. Phys. **48**, 530 (1977).
10. H. K. Wickramasinghe, Electron. Lett. **14**, 305 (1978).
11. W. Parmon, H. L. Bertoni, Electron. Lett. **15**, 684 (1979).
12. B. Hadimioglu, C. F. Quate, Appl. Phys. Lett. **43**, 1006 (1983).
13. J. Hildebrand, D. Rugar, J. Microsc. **134**, 245 (1984).
14. R. A. Lemons, C. F. Quate, Science **188**, 905 (1975).
15. D. Rugar, J. Appl. Phys. **56**, 1338 (1984).
16. J. Heiserman, Physica (Utrecht) **109 & 110B**, 1978 (1982).
17. J. Foster, Physica (Utrecht) **126B**, 199 (1984). □